Tribology Letters (2023) 71:54
https://doi.org/10.1007/s11249-023-01724-5

ORIGINAL PAPER

Wear Reduction via CNT Coatings in Electrical Contacts Subjected to Fretting

Bruno Alderete[1] · **Frank Mücklich**[1] · **Sebastian Suarez**[1]

Received: 24 January 2023 / Accepted: 22 March 2023 / Published online: 9 April 2023

Abstract

Carbon nanotubes (CNT) are of great interest to the research community due to their outstanding mechanical, transport, and optical properties. These nanoparticles have also shown exceptional lubricating capabilities, which coupled with their electrical conductivity show promising results as solid lubricants in electrical contacts. In this study, three different CNT coatings were deposited over copper platelets via electrophoretic deposition and subsequently tribo-electrically characterized including electrical contact resistance evolution during fretting wear, wear protection, chemical analysis of fretting marks, as well as influence of CNT coating thickness, duration and normal load applied during fretting, and atmospheric humidity. Thicker CNT coatings show improved wear protection while retaining similar electrical behavior as uncoated copper, or even improving its electrical contact resistance. Moreover, the compaction of the porous CNT coating is crucial for optimal electrical performance at low humidity. For longer fretting tests (150,000 and 500,000 cycles), the coatings are displaced thus affecting the wear protection offered. However, the coatings stabilize and reduce ECR compared to uncoated samples. Furthermore, thicker CNT coatings can bear higher loads during fretting due to the increased lubricant reservoir, with carbonaceous tribofilm remaining at the contacting interface after 5,000 fretting cycles regardless of normal load.

Graphical Abstract

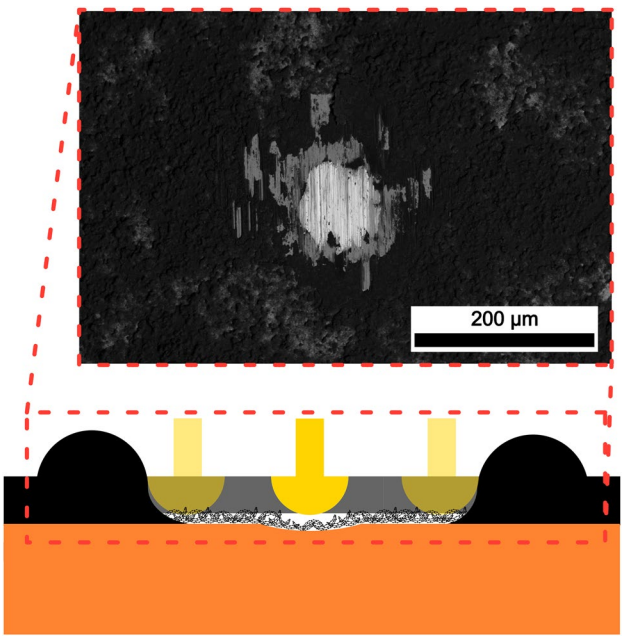

Keywords Carbon nanotubes · Electrical contact resistance · Fretting wear · Wear reduction

Extended author information available on the last page of the article

1 Introduction

Copper is widely used in electrical contacts due to its outstanding electrical conductivity, its moderate mechanical properties, its formability, along with its rapid passivation on account of its thin native oxide layer which is spontaneously formed when in contact with ambient conditions, and its low cost when compared with other contact materials—e.g., silver, gold, and platinum. As societal trends further move towards a more electrified future, it is crucial that more reliable, efficient, cost-effective, and more versatile electrical contacting systems are designed and developed [1–3]. In turn, this can not only increase material efficiency and reduce maintenance requirements in the systems, but also improve the overall sustainability of the electrical device.

Fretting wear is a phenomenon that can severely impact the duty life and optimal operation of electrical contacts. This does not only affect when in-operation, but also affects the reproducibility of a stable connection in separable contacts. Fretting occurs when two contacting bodies are in relative motion with one another. This motion is highly localized and of oscillatory nature [4, 5], with amplitudes typically ranging from a couple of micrometers up to 100 µm in electrical applications [5, 6]; however, fretting has also been studied in the nanoscale via techniques such as scanning probe microscopy [7]. Although fretting wear is not exclusive to electrical contacts, since all systems subjected to oscillatory motion can be affected, in this study we will focus on this specific application. The root of fretting wear cannot always be eliminated since it could be caused by mechanical vibrations intrinsic to the application—such as vibrations originating from an engine. Nonetheless, other sources such as dissimilar thermal expansion coefficient, mechanical shock, or electromagnetically induced vibrations can be—to a certain extent—mitigated by proper system and contact design [5, 8]. Environmental conditions can also impact fretting wear. Relative humidity in particular can affect the time it takes for electrical contact resistance (ECR) to stabilize while an electrical contact is subjected to fretting wear [5].

This wear mechanism degrades the contacting materials and entraps debris at the contacting sites, thus generating a considerable increase in electrical contact resistance [9]. When dealing with materials that form superficial films—e.g., copper and tin—the breakdown of these layers can be detrimental to the electrical behavior, but also in terms of wear resistance. Although the breakdown of copper oxide should increase the conductivity between the contacting bodies, the accumulation of debris could potentially hinder the electrical contact between the electrodes. Furthermore, the debris trapped at the contacting interface could act as third bodies, thus transitioning to severe abrasive wear.

As with other wear mechanisms, the effects of fretting wear can be minimized by proper lubrication of the contacting surfaces. In electrical applications, however, lubrication hinders the electron transport between the surfaces since it is an additional barrier. Furthermore, with some exceptions, most traditional lubricants possess high electrical resistivity, thus, imposing a significant increase in ECR. Consequently, liquid lubricants are not favored for electrical applications, hence opting for lubricant greases or solid lubricant alternatives. However, solid lubricants are not traditionally favored for fretting wear since these tend to be easily displaced, thus rapidly leaving the surface exposed to wear.

At an attempt to determine a more suitable solid lubricant alternative, four different carbon nanoparticles (CNP) coatings were investigated and tribo-electrically characterized [10]. From this study, we concluded that carbon black and carbon nanotubes (CNT) showed the most promising results based on their exceptional ECR behavior, as well as wear and oxidation protection, with CNT showing better results in general. Therefore, it is of interest to expand upon these results to further understand the lubricating capabilities of CNT coatings.

Carbon is a versatile element which is capable of forming different carbon–carbon bonds. The different bonds change the hybridization state of the carbon atoms, which in turn changes the properties of the formed allotrope [11–13]. The lubricating capabilities of allotropes such as onion-like carbon, carbon nanohorns, and CNT have been previously studied and reported [14–18]. However, for the specific application of electrical contacts, the conductivity of the carbon allotrope is of utmost importance. Therefore, CNT are a promising alternative since these CNP have not only been found to be exceptional solid lubricants, but these nanoparticles are also outstanding conductors [19–24], with a longer mean free path than copper and quasi-ballistic electron transport properties in metallic CNT [25–28]. This is important to keep in mind, since depending on the chirality of the CNT, these nanoparticles can behave as a metallic conductor or as a semiconductor [29–31]. Consequently, in this study, multi-walled carbon nanotubes (MWCNT) are used since they are easier to manufacture—compared to single-walled carbon nanotubes (SWCNT)—while having similar current carrying capacity as metallic SWCNT [32]. Furthermore, MWCNT present the added advantage that they conduct electricity as a zero band gap conductor since they always possess at least one metallic tube [33, 34].

Conventional solid lubricants, such as graphite and MoS_2, have specific humidity requirements in order to appropriately lubricate the contacting site. The former requires high atmospheric humidity—lower friction and wear at higher relative humidity—whereas the latter presents lower friction and wear at lower relative humidity [35, 36]. This humidity-dependent behavior has been widely reported for graphite.

Multiple models have been proposed—e.g., Savage, Rowe and Bryant, Bollmann and Spreadborough, among others—however, authors agree that graphite is not an intrinsically good lubricant, but rather requires ambient moisture to become one [37–42]. However, it is now understood that water's role in graphite's lubricity is not physiosorbed but rather dissociative chemisorption, thus leading to the formation of H and OH ions [37, 43]. Moreover, recent work by Morstein et al. suggest an extended adsorption model due to the tribo-induced formation of turbostratic carbon [38]. This structural transition enables graphite to lubricate even at high loads and low humidity.

A review article from Kumar et al. has summarized the temperature range of applications of different solid lubricants [44]. In their study, the authors have placed graphite and other carbon materials—such as diamond-like carbon and CNT—in similar working ranges. Therefore, it is of great interest to evaluate the influence of atmospheric moisture on the wear protection offered by CNT coatings. It is hypothesized that humidity will not have a significant influence on the lubricating capabilities of this CNP due to the sp^2-hybridization state of CNT, coupled with the large aspect ratio of the tubes themselves (1-dimensional material) [45]. Therefore, it was hypothesized that CNT lubricate by rolling on the surface, thus acting like a roll bearing [15, 46, 47]. However, if that were the case, friction would be significantly lower than what is usually reported [14, 46]. New research by MacLucas et al. has demonstrated that the main lubrication mechanism active in CNT is sliding rather than rolling [48].

Within the scope of this work, CNT will be deposited via electrophoretic deposition (EPD) over copper substrates [13, 49, 50], followed by tribo-electrical characterization via fretting tests and ECR measurements [10]. The fretting tests were carried out at constant normal load, with periodic ECR measurements at set intervals (static ECR) to track the evolution of ECR as fretting tests progress. Three different coating thicknesses were evaluated, as well as four different normal loads to gather insight into their respective influences on wear and electrical behavior. Fretting tests were also conducted at low relative humidity to analyze the potential use of CNT coatings as lubricants even in the absence of atmospheric moisture. The resulting fretting marks were subsequently characterized via confocal laser scanning microscopy (CLSM) to determine the affected area, as well as scanning electron microscopy (SEM) to micrograph the fretting mark. Furthermore, chemical analysis via energy dispersive X-ray spectroscopy (EDS) was conducted to acquire information on the oxidation state of the fretting mark, as well as to quantitatively assess material transfer from the counter electrode onto the coated electrode, done by the acquisition of elemental mappings.

2 Materials and Method

The substrates used were laminated, flat, oxygen-free, pure-copper platelets (25 × 10 × 1) mm (Wieland Electric GmbH, Germany). These copper platelets were ground (P1200 grit silicon carbide grinding paper) and polished at 6, 3, and 1 µm to obtain a mirror-polished surface before coating; thus achieving a root mean square roughness between 10 and 20 nm. The CNT used were chemical vapor deposition (CVD)-grown MWCNT (Graphene Supermarket, USA). The outer diameter of the CNT have a distribution between 50 and 85 nm, an as-received state length from 10 to 15 µm, and a carbon purity above 94%.

Potentiostatic EPD was carried out at a set voltage of 300 V, with an inter-electrode distance of 15 mm. The dispersion parameters and deposition process were thoroughly explained in Alderete et al. [10, 13, 49, 50]. Three different CNT coatings were produced, where the only parameter that was varied was the deposition time—i.e., the coating thickness [10, 13]. Therefore, a total of four samples were analyzed, namely: an uncoated copper reference sample, and three CNT-coated samples with deposition times of 3, 4, and 5 min (henceforth CNT3, CNT4, and CNT5, respectively).

After coating the samples were tribo-electrically characterized via a custom multipurpose testing rig [51]. This setup allows an ample combination of tribological and electrical characterization. In this work, we focus specifically on conducting fretting wear tests with periodic ECR measurements at set intervals (static ECR) to evaluate the influence of CNT coating thickness, normal load applied, as well as ambient humidity and test duration. Since this report follows up on previous work [10], it is of interest to maintain the same fretting parameters to ensure comparability. Contrarily, changing a parameter might influence the results. For example, it was reported by Park et al. that varying the amplitude of fretting tests affects the resulting dynamic ECR [52]. The authors also analyze different permutations of frequency and amplitude and show the resulting fretting mark, as well as

Table 1 Summary of tribo-electrical testing parameters

Measurement	Load/N	Fretting cycles /10^3 cycles	Intervals /10^3 cycles	Relative humidity
1	0.5	5	0.1	30–40%
2	1			
3	2.5			
4	5			
5	1			15%
6		150	1	30–40%
7		500		

reporting the time it takes for ECR to stabilize with the different parameter combinations [52]. Therefore, in our study, fretting tests were conducted with an amplitude of 35 µm and an oscillation frequency of 8 Hz, matching those of our previous work [10].

ECR measurements were conducted using the four-probe method sourcing a direct current of 100 mA using a Keithley 2400 SMU. This current level was chosen to stay under dry-circuit conditions [53]. The voltage drop was measured using a Keithley 2182a nanovoltmeter with a voltage range of 1 V. The contacting counter electrode for fretting and ECR measurements was a silver-nickel core ($AgNi_{0.15}$) hard-gold-coated ($AuCo_{0.2}$) rivet (Adam Bornbaum GmbH). These rivets have a curved head, with a mean diameter of curvature of 4 mm and a root mean square roughness of 0.25 µm. The hard-gold coating has an average thickness of 6.47 ± 0.18 µm. In the loading ranges evaluated in this study (0.5–5 N), a maximum Hertzian contact pressure between 314 and 676.5 MPa is achieved. All atmospheric tribo-electrical tests were carried out at ambient conditions, i.e., temperature and humidity ranging from 20 to 25 °C and 30–40% r.h., respectively. The low humidity tribo-electrical measurements were conducted using a climate test chamber set at 20 °C and 15% r.h. Seven different fretting conditions per sample were evaluated, summarized in Table 1. Ten ECR measurements were carried out before fretting as well as at each cycle interval and then averaged, with each fretting test being reiterated at least three times. A new rivet was used for every measurement.

After tribo-electrical testing the fretting marks were imaged with SEM (using ETD detector and 5 keV acceleration voltage) and chemically analyzed via EDS (ThermoFisher Helios™ G4 PFIB CXe DualBeam™ FIB/SEM equipped with an EDS detector EDAX Octane Elite Super). EDS scans were carried out using an acceleration voltage of 15 keV, thus acquiring a 2-dimensional chemical distribution map. Topographical and wear analyses were carried out by imaging via CLSM (LEXT OLS4100, Olympus) using a laser wavelength of 405 nm. A larger field of view at higher resolution was attained by stitching a 2×2 or 3×3 grid (depending on wear track size) at $50 \times$ with a 20% overlap. With the information acquired via CLSM scans coating thickness, worn area, and roughness after fretting can be obtained.

A 5×2 grid at $50 \times$ was stitched in the CLSM to measure coating thickness. The coatings have an average thickness of 1.27 ± 0.12 µm, 1.62 ± 0.11 µm, and 1.77 ± 0.01 µm for CNT3, CNT4, and CNT5, , respectively.

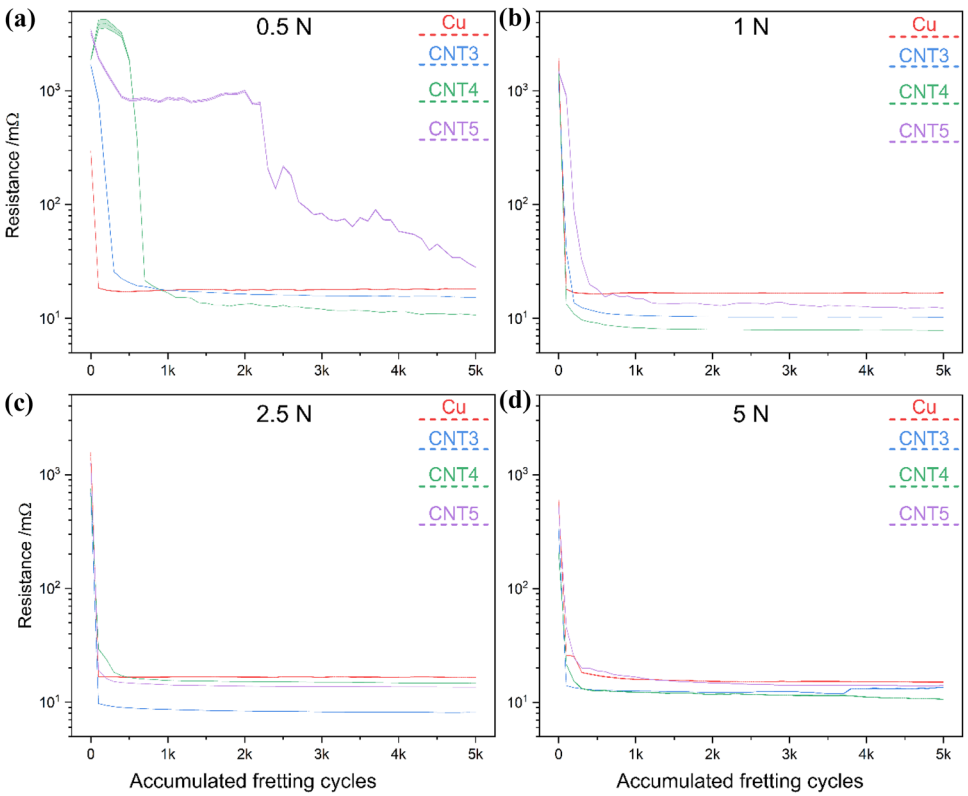

Fig. 1 ECR measurements of CNT-coated samples for a total of 5 k fretting cycles at **a** 0.5 N, **b** 1 N, **c** 2.5 N, and **d** 5 N. The line plot indicates the tendency of the ECR evolution during static ECR measurements

3 Results and Discussions

3.1 Electrical Behavior

3.1.1 Influence of Normal Load

The ECR evolution based on the analyzed normal loads are shown in Fig. 1. These fretting tests were all carried out for a total of 5 k cycles with periodic ECR measurements every 100 cycles. It is noteworthy to highlight that these measurements are highly reproducible, with very low error—standard deviation of the measurements are plotted in all ECR curves, however these cannot be appreciated due to the thickness of the line itself. Furthermore, it should be noted that since static ECR was measured, the line plot shows the ECR tendency and not the actual behavior. Observing the plots from Fig. 1 it can be seen that the behavior of the uncoated copper substrate is consistent regardless of normal load. The ECR value of the reference prior to fretting are high, however, after the first 100 fretting cycles the ECR value sharply decreases to approximately 20 mΩ and remains constant throughout the measurement. The behavior is unexpected, since the breakdown and reformation of the oxide layer should cause fluctuations in the resistance between intervals. However, due to the short period of time between consecutive ECR measurements—it takes approximately 20 s for the setup to complete 100 cycles—the thickness of the reformed oxide layer could not be sufficient to affect the resistance. This behavior could also be associated with the number of a-spots being established and remaining constant throughout the fretting cycles, consequently presenting constant ECR.

Focusing on the tests done at 0.5 N, CNT5 stands out from the rest. This coating presents an initial reduction in ECR during the first hundred cycles caused by the compaction and adjustment of the coating during fretting. The ECR remains constant for the following couple thousand cycles, followed by a progressive reduction in ECR. The sudden reduction at around 2 k cycles could be due to (1) the breakdown of a large CNT agglomerate at the contacting site, or (2) the displacement of a significant portion of the CNT coating. Based on the observed behavior, the former seems more likely. Following the fretting-induced breakdown of the CNT agglomerate, smaller agglomerates are subsequently displaced from the fretting mark; thus explaining the progressive reduction in the following fretting cycles.

Initially, CNT4 shows similar behavior as CNT5. However, after 500 cycles the ECR sharply falls to values that approach that of the uncoated reference. As the fretting cycles progress, a small reduction in ECR is observed, with values falling below that of the copper reference and reaching values of approximately 10 mΩ. CNT3 behaves akin to the uncoated reference, with ECR values falling below 30 mΩ after a few hundred cycles. After 1 k cycles, CNT3 presents lower ECR than the uncoated reference, however, the resistance is still higher than that of CNT4.

When increasing the normal load, the ECR behavior tends to not vary as considerably as with low normal loads—i.e., 0.5 N. In the tests carried out at 1 N, 2.5 N, and 5 N, ECR values quickly fall below 30 mΩ and outperform the uncoated reference within the first 1 k cycles. CNT5 shows improved performance compared to the uncoated reference sample, however, the thinner three- and four-minute coatings consistently outperform the thickest coating.

The normal load during fretting does not have an observable influence on the ECR of an electrical contact. This was evidenced by the uncoated reference sample, and corroborated with the coated samples from normal loads above 0.5 N. The considerable deviation in the coated samples at 0.5 N is a consequence of inadequate electrical contact in the system. At low loads, the coating is not sufficiently compacted, thus presenting a porous network that hinders electron transport from the counter electrode towards the substrate. Furthermore, thicker coatings require more fretting cycles to breakdown the larger CNT agglomerates, thus initially presenting higher ECR values. When contacting at

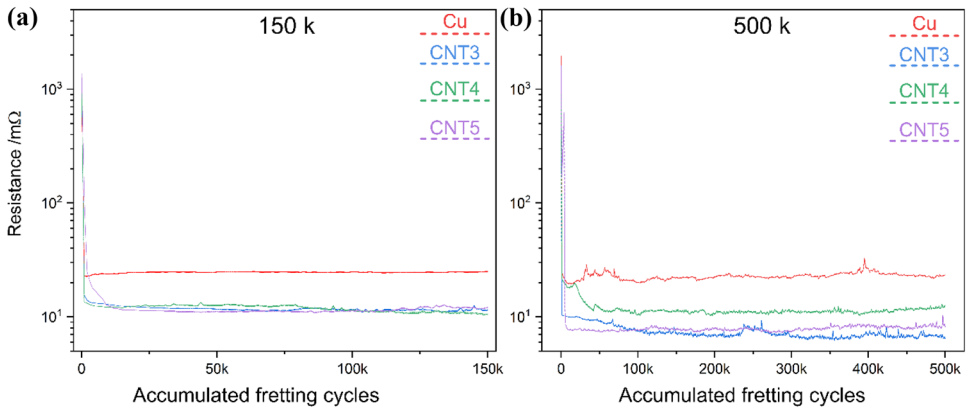

Fig. 2 ECR measurements of CNT-coated samples at 1 N for a total of **a** 150 k and **b** 500 k fretting cycles. The line plot indicates the tendency of the ECR evolution during static ECR measurements

higher normal loads, these elevated contact pressures, coupled with the oscillatory motion, enable the breakdown of these agglomerates at a much faster rate. Consequently, the resistance values stabilize reaching a steady state with fewer fretting cycles.

It is, therefore, crucial that thin coatings are employed in electrical contacts that operate at low normal loads. Contrarily, undesired energy loss will take place at the contact interface, thus lowering its efficiency. When the contact operates at higher normal loads, on the other hand, the coating thickness is irrelevant. However, to optimize material efficiency, a three-minute CNT coating is sufficient from an electrical perspective.

3.1.2 Endurance Test

The electrical behavior of the samples at 1 N for longer fretting durations is shown in Fig. 2. As was the case for 5 k cycles (Fig. 1) the ECR value of the uncoated reference tends to stabilize at approximately 20 mΩ. In the case of the 500 k-cycle test slight fluctuations are observed. Regardless of the variation observed, the value does not vary past 30 mΩ—values which correlate with those measured in the 150 k-cycle test.

In the longer fretting tests the coatings show a considerable improvement in terms of contact resistance. Regardless of coating thickness, the ECR values are half of that of the uncoated sample, or even lower. It was initially believed that longer fretting tests could be more severely influenced by the breakdown and subsequent reformation of the oxide layer. However, this is proven otherwise since the ECR values of the uncoated reference resemble those of the references in the shorter fretting tests. Nonetheless, the presence of a thin copper oxide layer that forms between ECR intervals cannot be disregarded. These tests are conducted with intervals that last over four times more than the shorter tests, however, the duration is still relatively short. Therefore, a complete reformation of the oxide layer is unlikely since the spontaneous formation of Cu_2O takes considerably longer [54].

Furthermore, as opposed to what was observed for shorter fretting tests (Fig. 1), the thickness of the coating does not have a significant influence on the electrical behavior of the coated samples. The five-minute CNT coating performs on par with the thinner coatings, all outperforming the uncoated reference. It seems that the carbonaceous tribofilm formed enhances the electron transport at the interface.

3.1.3 Influence of Ambient Humidity

The influence of humidity on the electrical behavior of metals when subjected to fretting wear has already been analyzed by Timsit and Antler (in Slade) [5]. In their work, the authors report that at lower ambient humidity, copper

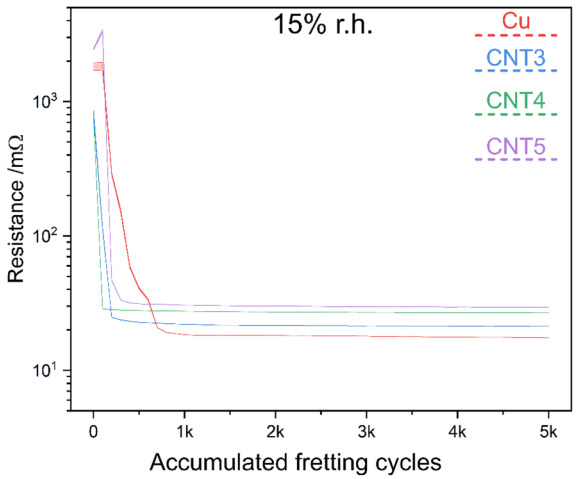

Fig. 3 ECR measurements of CNT-coated samples for a total of 5 k fretting cycles at a constant temperature and humidity (20 °C and 15% r.h., respectively). The line plot indicates the tendency of the ECR evolution during static ECR measurements

electrical contacts show an improved duration when subjected to fretting wear. In other words, the copper contact requires considerably more fretting cycles to reach the ECR threshold of failure proposed by the authors. Therefore, it could be foreseen that the uncoated copper shows higher ECR values at lower fretting cycles, stabilizing after 700–800 cycles. After stabilization, the copper reference shows ECR values that resemble the measurements carried out at ambient conditions (see Fig. 3). The coated samples, on the other hand, reach a steady state rather quickly, after around 300 cycles. However, the steady state values of the coated samples are of interest since now the uncoated reference outperforms the coated samples. Under these conditions thicker coatings promote higher ECR values. Although the increase is marginal, the tendency is clear. This behavior was not expected since it has been previously reported that metallic SWCNT show the opposite behavior—i.e., resistance increases as relative humidity increases [55–57]. Since MWCNT always have a conductive tube, it was expected that resistance would decrease at lower humidity. However, this humidity-dependent behavior was reported for humidity sensing devices. In our analysis a more complex scenario is taking place due to the addition of tribological testing.

The worsened electrical behavior of the coated samples could be associated to a tribologically induced degradation of the CNT, however, this is unlikely on account of the longer fretting tests carried out (see Fig. 2). As witnessed in the 150 and 500 k cycle tests, the ECR of the coated samples outperform the uncoated reference despite the greater stresses incurred onto the CNT. Therefore, it is implausible that at 15% r.h. and 5 k fretting cycles more severe wear took place in the CNT rather than in 150 k and 500 k cycles.

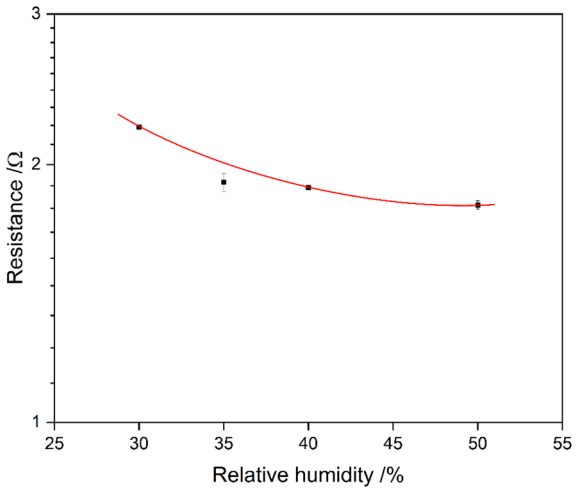

Fig. 4 ECR of CNT4 at different humidity with second order polynomial fitting (r-square = 0.991)

To confirm the tribological-independence of the ECR gain, static-constant-load ECR measurements at 1 N were carried out with the same instrumental parameters as with the tribo-electrical tests. Four different ambient humidity conditions were evaluated (i.e., 30, 35, 40, and 50%), measured at five different points in CNT4 with twenty measurements per point—giving a total of 100 ECR measurements per r.h. These values were then averaged and plotted, shown in Fig. 4. As the graph illustrates, it is clear that higher r.h. promotes lower ECR values. Therefore, the electrical behavior observed in Fig. 3 is not caused by the tribological tests but rather is inherent to our coating systems. Although the literature suggests that CNT should show the inverse behavior, it is important to highlight that our system differs significantly from those previously studied—i.e., studies on resistive CNT-based humidity sensors. In a study by Lee et al. they used SWCNT networks analyzing the electrical response of metallic and semiconducting CNT [56], whereas Ling et al. worked with thin SWCNT networks with thicknesses below 1 µm [57]. On the other hand, highly dispersed and aligned MWCNT have been used by Tsai et al. as sensor interconnections [55]. The CNT coatings dealt with in this study differentiate themselves from those previous studies in the following ways:

- The coatings are made up of a composition of individual CNT and CNT agglomerates, with a mean agglomerate area fraction of approximately 43% [50].
- The coatings are highly porous, thus requiring pressure from the counter electrode to compact and adjust internally to reduce ECR by increasing the amount of parallel percolation paths—see focused ion beam cross sections in [13].

The latter is believed to play a crucial role in the humidity-dependent behavior of the CNT coatings. It is hypothesized that ambient humidity promotes lower ECR values since moist air is a better electrical conductor than dry air. Therefore, the dry air found in the porous network of the CNT coatings influences the ECR behavior, possibly explaining the electrical behavior of the CNT-coated samples from Fig. 3.

Another phenomenon that could influence the electrical behavior at higher atmospheric humidity is that of electrowetting [58]. The contact angle of a water droplet can be modified in the presence of an electric field [58, 59], causing the droplet to become more hydrophilic (flatten out) when a voltage is applied and showing its most hydrophobic state in the absence of an electric field. Although the voltages that the authors report are significantly higher than the voltages recorded in our ECR measurements, this flattening effect could improve the contact between individual CNT and CNT agglomerates by bridging the voids in the coating even further—in addition to compaction due to the normal load applied—thus improving the system's conductivity at higher humidity levels. Furthermore, the small dimensions of the CNT and CNT agglomerates, coupled with their curvature, could potentially intensify this effect by concentration the electric field thus causing the flattening of moisture droplets even at low voltages. Moreover, the small dimension of moisture droplets—as opposed to macro-sized droplets—would require lower voltages to change its wetting behavior.

Therefore, although there is an increase in ECR at low humidity, these coatings could still be beneficial in applications where the ambient humidity varies over time. For specific applications operating for prolonged periods of time at low humidity, on the other hand, the negative influence on the electrical behavior of the CNT coatings is counterproductive, thus promoting loss in contact efficiency. However, it should be noted that 15% r.h. is a low atmospheric value, with higher typical values in central Europe [60, 61]. The wear protection offered should be carefully analyzed to evaluate if the wear reduction offered at low ambient humidity could outweigh the gain in ECR.

3.2 Wear Protection

3.2.1 Influence of Normal Load

SEM micrographs of the fretting marks for each sample at each load are shown in Fig. 5, with the red dashed line highlighting regions where severe wear took place, i.e., gross slip [62]. Only regions where gross slip took place are considered for the relative worn area calculations. Observing the

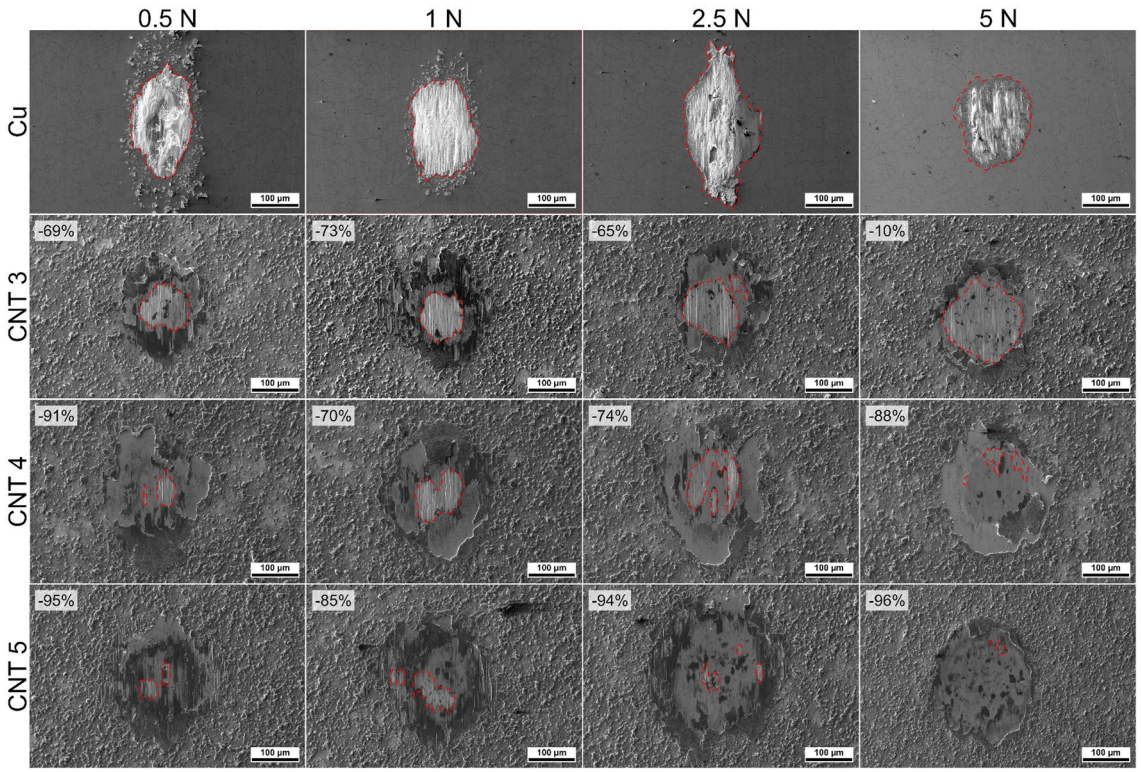

Fig. 5 SEM micrographs of fretting marks after 5 k fretting cycles. The red dashed lines highlight the areas where severe wear is observed (gross slip). The number at the top left corner of each CNT-coated sample exhibits the reduction in worn area relative to the respective uncoated copper sample

load-dependent behavior of the uncoated copper sample, two aspects stand out: (1) the wear track tends to decrease in size as the load increases, with the 5 N fretting mark showing the smallest worn area, and (2) formation of debris surrounding the fretting mark is only observed for load below 2.5 N. The latter is of concern from a tribological standpoint since debris can be trapped at the contacting site, thus causing third-body abrasion. This phenomenon, coupled with adhesive wear, could further promote the transition from mild to severe wear [63]. The lack of loose debris formation at 5 N exemplifies this behavior. Since debris are not prominent in this fretting mark, the only wear mechanism active is adhesive wear and two-body abrasive wear. The latter, however, is not as dominant in the system due to the soft radius of curvature of the counter electrode. Therefore, in this case, three-body abrasive wear due to debris formation is more detrimental rather than two-body abrasion. Although debris pile up can be observed at 2.5 N, these particles are located at the ends of the fretting tracks. Therefore, the particles are displaced onto the upper and lower limits of the oscillatory motion, thus reducing the likelihood of third-body abrasion. The geometry of the counter electrode also explains the smaller worn area at higher normal loads. The non-conformal contact established between the bodies implies a considerably higher contact pressure at the tip of the rivet, which, in turn drastically increases frictional forces. Furthermore, metallic oxides generally have higher shear strength than the unoxidized metal. Therefore, according to Tabor's theory [36], higher shear strength also causes higher friction. Higher friction restricts, to a certain extent, the displacement of the counter electrode over the copper surface. Consequently, the load is more concentrated on the central part of the amplitude of motion, thus causing smaller worn areas.

The fretting marks of the CNT-coated substrate look notably different compared to their uncoated counterparts. The wear tracks are smaller, as evidenced by the relative worn area reduction at the top left corner of each micrograph. Although coating displacement is observed, with the micrographs showing exposed regions of the substrate as well as clusters of CNT agglomerates surrounding the fretting mark. The degree to which the coating is displaced varies from sample to sample; however, it was observed for all coatings. Nonetheless, coating displacement does not appear to affect the wear protection offered by the CNT coating. Certain fretting marks showing severe displacement, and even coating removal such as CNT4 at 2.5 N still offer considerable wear protection compared to the uncoated reference, with a worn

area that is over 70% smaller than the copper sample at 2.5 N—areas measured from CLSM scans.

At and below 2.5 N CNT3 shows considerable wear protection, with a worn area that is between 60 and 70% smaller compared to their uncoated counterparts. At 5 N, however, there is a marginal reduction of the worn area at only 10%, approximately. Nonetheless, the damage incurred at 5 N in the coated sample does not appear as severe as the uncoated sample.

CNT4 and CNT5 show exceptional wear protection. In all cases a reduction in the worn area of at least 70% can be observed, regardless of normal load and state of the coating—i.e., coating damage and/or displacement/piling up. For these two coatings, fretting at 5 N does not incur considerable damage onto the substrate's surface, showing partial slip rather than gross slip as in the uncoated reference. In fact, CNT4 and CNT5 at 5 N show the least amount of damage after 5 k cycles. This is attributed to the lack of debris formation, as well as CNT clusters that remain at and around the contact site after the fretting cycles, evidenced by the black regions in the SEM micrographs—and later verified by EDS mappings. This is especially true for all measurements carried out on the CNT5 sample. Due to the considerably thicker coating, an abundance of CNT remains at the contacting interface, thus granting greater wear protection throughout the measurement cycles.

Furthermore, the electrical behavior of CNT5 at 0.5 N is reasonable observing the SEM micrograph (see Fig. 1a). This image shows a significant amount of CNT remaining at the contacting site. Although this is extremely desirable from a solid-lubrication perspective, it is important to note that CNT are not as conductive as the metallic electrodes—despite the fact that individual CNT demonstrate exceptional electron transportability.

With sufficiently thick CNT coatings, the wear protection offered is independent of the normal load during fretting. Some variations are observed; however, this is intrinsic to the heterogeneity of the coatings themselves [13]. Contrarily, the thinner CNT3 coating shows a substantial increase in worn area at 5 N, resembling the uncoated sample. At lower loads, some wear protection is offered, however, it is not as significant as in the thicker coatings. Consequently, a coating thickness threshold is established, with a requirement of at least 1.5 to 1.6 µm to observe consistent and load-independent wear protection.

From a tribological standpoint, thicker CNT coatings are more desirable since they offer a larger lubricant reservoir. As evidenced by the micrographs from Fig. 5, thicker CNT coatings provide a more significant wear protection, with CNT remaining at the contact site after tribological testing. However, when taking into account the purpose of these coatings, thicker coatings may be counterproductive.

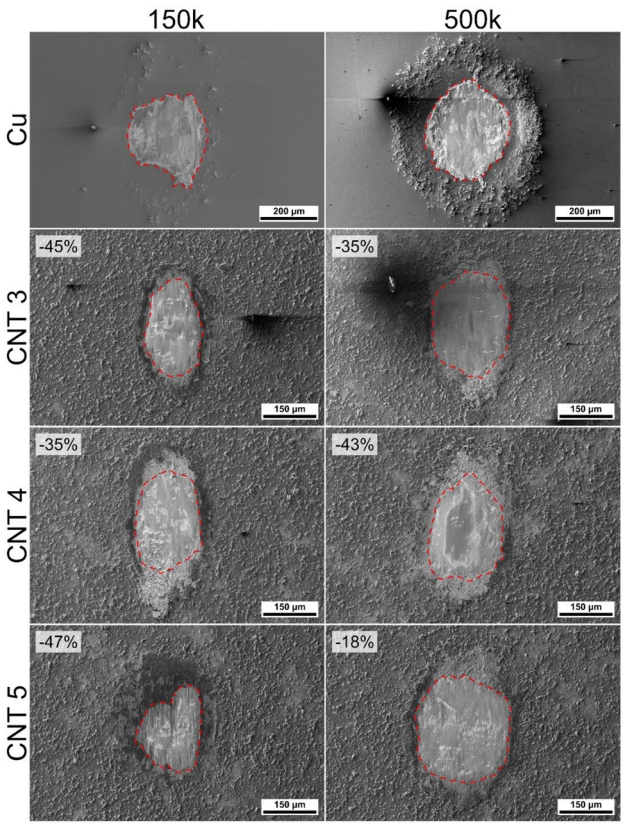

Fig. 6 SEM micrographs of fretting marks after 150 and 500 k fretting cycles. The red dashed lines highlight the areas where severe wear is observed (gross slip). The number at the top left corner of each CNT-coated sample exhibits the reduction in worn area relative to the respective uncoated copper sample. Note that the magnification of the uncoated samples is smaller than the magnification of the coated samples

In other words, for electrical applications, thicker coatings have a more significant impact on the conductivity of the system. Therefore, a tradeoff must be considered, where a balance between wear protection and admissible ECR gain must be weighed.

3.2.2 Endurance Test

The SEM micrographs resulting from the 150 and 500 k fretting cycles tests on the coated and uncoated samples are shown in Fig. 6. As expected, the uncoated samples show substantial wear after 500 k cycles. Since these tests were carried out at 1 N—and based on the behavior of the substrate after 5 k cycles—it was also expected that debris would gather around the fretting mark. However, the amount of debris observed around the 500 k cycles is significant. After 150 k cycles, on the other hand, a negligible amount of debris is observed, especially when compared to the 500 k cycles measurement. These tracks are significantly larger than the 1 N tracks after 5 k cycles, with the 150 k

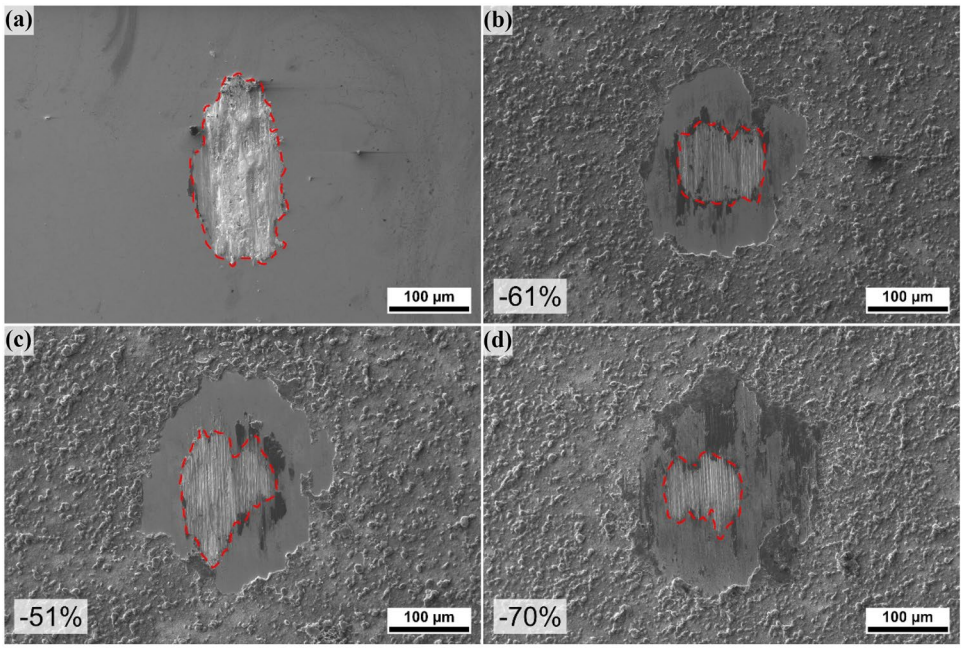

Fig. 7 SEM micrographs of fretting marks after 5 k fretting cycles at 20 °C and 15% r.h. **a** Uncoated copper, **b** CNT3, **c** CNT4, and **d** CNT5. The red dashed lines highlight the areas where severe wear is observed (gross slip). The number at the bottom left corner of each CNT-coated sample exhibits the reduction in worn area relative to the respective uncoated copper sample

cycles track being double the size and the 500 k cycles track three-fold the size of the 5 k track. For this reason, the magnification of the micrograph had to be reduced. The same can be stated about the CNT-coated samples, with these representing an even larger multiple compared to their 5 k counterpart.

The micrographs of the CNT-coated samples reveal that CNT are not as effective in reducing wear after prolonged fretting cycles, showing gross slip regardless of coating thickness. Although all coatings show a reduction in worn area, the degree to which the coatings reduce wear is not as significant as was the case in shorter fretting cycles. This is because the CNT are displaced from the contact site, thus eliminating the possibility of reducing wear. Therefore, for prolonged fretting cycles, the wear reduction capability of CNT is irrespective of the coating thickness since the nanoparticles are displaced from the contacting interface altogether.

Even though the coatings do not perform as exceptionally well for prolonged fretting cycles in terms of wear protection, they do improve the electrical behavior of the system—see Fig. 2. Therefore, their potential use for electrical systems should not be discarded. All three coatings outperform the uncoated reference, with low and stable ECR throughout the entire measurement. Although wear protection is sparse, the electrical advantage is beneficial.

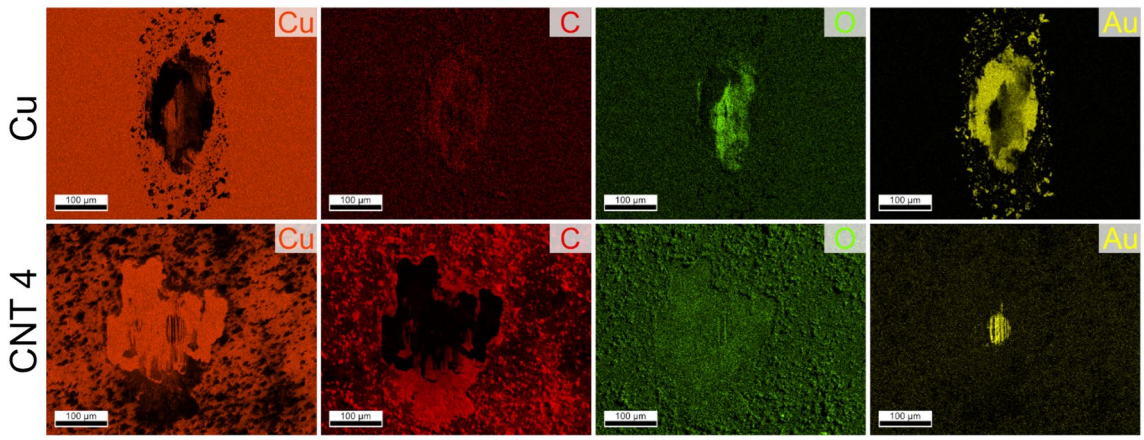

Fig. 8 EDS maps of uncoated copper and CNT4 showing copper, carbon, oxygen, and gold after 5 k fretting cycles at 0.5 N. EDS maps of all fretting marks are available in the Online Resources

3.2.3 Influence of Ambient Humidity

The SEM micrographs of the fretting tests carried out at low humidity are shown in Fig. 7. The worn area of the uncoated reference after 5 k cycles at 1 N from Fig. 5 is comparable with the size of the reference at 15% r.h. However, in the case of the coated samples, all coatings show an increase in worn area as a consequence of the lower atmospheric humidity. The increase in relative worn area is linked to the coating thickness, with thicker coatings showing worse wear protection compared to thinner coatings. Therefore, it is established that CNT, similarly to graphite, requires moisture to reduce wear. As the tubes degrade as a consequence of severe stress, they start to break apart into individual graphite and graphene sheets. The tubes' degradation into graphite-like structures justifies the more severe wear observed in the SEM micrographs [64]. For this function, MWCNT are better suited than SWCNT since MWCNT require higher pressures to break their bonds and degrade the tubes into graphitic structures. Furthermore, the degradation of MWCNT—as opposed to SWCNT—would provide a more ample source of graphitic structures, thus improving lubricity to a certain extent. Consequently, the MWCNT employed in this study continue demonstrating wear protection at low humidity levels after 5 k fretting cycles, with worn area reductions of at least 50% compared to the reference sample.

3.3 Chemical Analysis

EDS was carried out to qualitatively determine the chemical composition of the fretting marks. The resulting EDS maps of the fretting marks conducted at 0.5 N and 5 k cycles for the copper reference and CNT4 are shown in Fig. 8. Although EDS maps for all conditions and samples were acquired, only these two fretting marks will be discussed in this section since similar behavior was observed throughout the remaining fretting marks. EDS maps of all samples analyzed at 0.5 N, 1 N, 2.5 N, and 5 N are shown in Online Resource 1, 2, 3, and 4, respectively. Online resource 5 shows the EDS maps of fretting marks after tests at 15% r.h. of all samples, whereas Online Resources 6 and 7 show the fretting marks after 150 k and 500 k, respectively.

A key takeaway from the EDS maps of the uncoated copper sample is that oxidation takes place during fretting, as evidenced by the spike in oxygen intensity at the center of the wear track. Furthermore, it is of interest to highlight the extent to which gold was transferred from the counter electrode towards the copper sample. As evidenced, almost the entirety of the fretting mark contains gold. In addition, the debris observed in the SEM micrographs (Fig. 5) is purely made up of gold, as proven by both the copper and gold intensity maps. This implies that material is supplied to the copper sample rather than material being purely removed by fretting. The transfer of gold is promoted by the harder counterpart—i.e., the oxide layer—since dissimilar hardness between the contacting surfaces fosters material transfer from the softer onto the harder surface [5, 6]. The removal of the softer material and its deposition onto the harder material is caused by the sliding motion, where asperity junctions are stronger than the weaker metal. Moreover, the continuous breakdown of the re-formed oxide film due to fretting wear further favors the adhesion of gold onto the copper surface [6]. As fretting cycles progress, gold continuously adheres to the copper sample and is subsequently removed from the wear track, resulting in gold debris surrounding the contacting site. Nonetheless, recalling the SEM micrographs from Fig. 5, the formation of debris was only observed at normal loads below 2.5 N and for prolonged fretting cycles, primarily 500 k cycles.

The EDS map of CNT4 shows some decisive differences compared to the copper sample. Copper is more homogeneously distributed in the coated sample. Here, regions where copper is not detected is caused by the thickness of the coating which hinders the emitted x-ray from the base material from reaching the detector. Accordingly, carbon intensities are maximum in sites where copper is not detected, and vice versa. Another key difference is the degree of oxidation incurred onto the copper substrate during fretting. Observing the oxygen map closely, no spikes in intensities can be identified. Therefore, the oxygen detected is found either in the copper's surface—in the form of Cu_2O—or as functional groups bound to the nanotubes. The last distinction is the amount of gold that is transferred. Although EDS is a qualitative technique, the signal-to-noise ratio of gold in CNT4 shows that the maxima in gold are not as strong as is the case in the uncoated sample. Furthermore, the gold that is transferred onto the copper sample is concentrated at the center of the fretting mark. Moreover, gold debris is not formed in the CNT-coated sample as a consequence of the lubricity of the nanoparticles, thus reducing gold's adhesion. These distinctions between uncoated and CNT-coated samples are consistent throughout all fretting marks regardless of test parameters or coating thickness.

The carbon map of CNT4 also shows the presence of carbonaceous phase remaining in the contact area even after 5 k cycles regardless of coating displacement, thus explaining the reduction in worn area of the coated samples. This is the case in all CNT-coated samples, except for prolonged fretting cycles where the coating is entirely displaced from the contacting site (see Online Resources 6 and 7). This fact explains the milder wear protection offered by the coatings after 150 k and 500 k fretting cycles. As a consequence of the coating displacement, the coated samples show similar

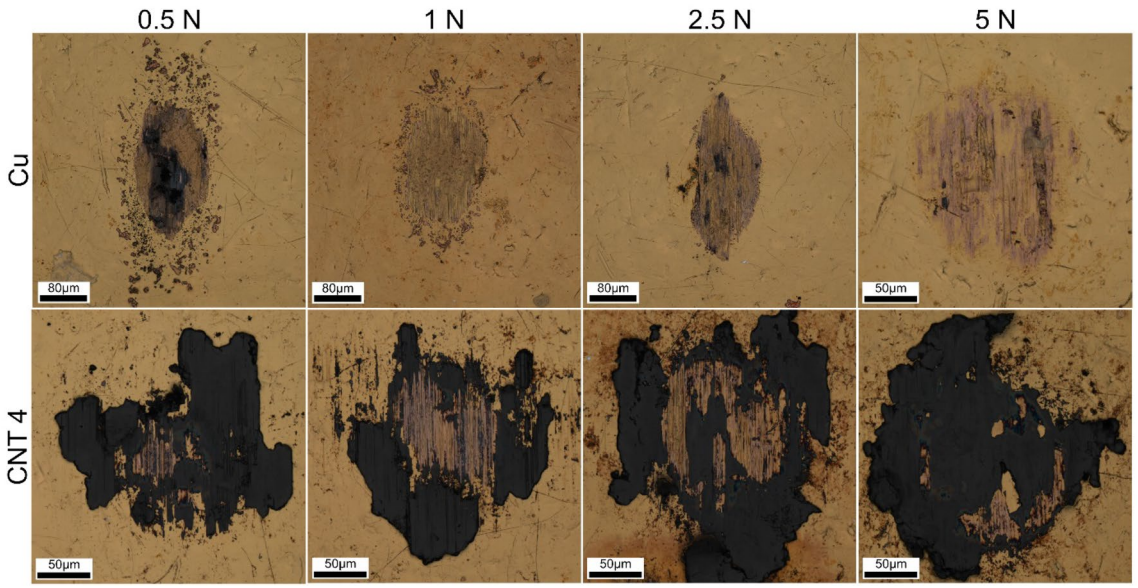

Fig. 9 CLSM light scan of counter electrode used against copper and CNT4 for the different loading conditions and 5 k fretting cycles. CLSM scans of all fretting marks are available in the Online Resources (including light, laser and height)

degrees of oxidation and gold transfer—as well as gold debris formation—as their uncoated counterparts.

3.4 Counter Electrode

CLSM scans of the counter electrode after fretting were carried out, with Fig. 9 showing the damage incurred under different loading conditions when contacting against uncoated copper and CNT4. For the light, laser, and height scan of all fretting marks refer to the Online Resources. CLSM scans of the counter electrodes used at 0.5 N, 1 N, 2.5 N, and 5 N are shown in Online Resources 8, 9, 10, and 11, respectively. The scans for counter electrodes used on fretting tests done at 15% r.h. are shown in Online Resource 12, with Online Resources 13 and 14 showing the counter electrodes after 150 k and 500 k fretting cycles, respectively.

As Fig. 9 shows, gold debris surrounds the fretting mark on the counter electrode that contacted the uncoated sample at 0.5 N as well as 1 N, concurring with the observations of the uncoated copper electrodes. Furthermore, the affected regions in the counter electrode dimensionally resemble the observations on the counter electrode, with higher loads showing smaller areas where gross slip took place. The CLSM scans also show that there is no material transfer from the uncoated electrode towards the counter electrode. The unidirectional transfer of material from the gold counter electrode towards the uncoated copper is due to the hardness difference between the contacting surfaces. In order for bidirectional material transfer to take place, the contacting surfaces should possess a hardness difference below 10% [5]. Since the hardness of the counter electrodes is 1.36 ± 0.01 GPa (measured via microhardness measurements on Struers Inc. Dura Scan with a load of 0.98 N), whereas—according to literature—copper oxide thin films have a hardness between 7.2 ± 0.2 GPa and 12.3 ± 0.5 GPa, depending on grain size [65]. Moreover, as the oxide layers are broken by the progression of fretting tests, the contact between the "clean" surfaces improves adhesion of the metallic surfaces due to the strengthening of the interfacial bonds between the contacting asperities [6].

The scans conducted on the coated samples are of considerable interest since these prove that carbon was transferred onto the counter electrodes. This is significant since the uncoated regions in the contacting site (shown in the micrographs in Figs. 5, 6, and 7) are not areas where the coating was removed, but rather there was a relocation of the coating from the copper substrate towards the gold rivet. This was seen in all the CNT coatings to varying degree; variations caused by inherent heterogeneity of the coatings. Nonetheless, carbon transfer was consistently observed on the counter electrodes regardless of coating thickness (see Online Resources 8–14).

Carbon transfer is not only load independent, but also humidity independent, with CNT being observed on the counter electrodes on all tests conducted at 15% r.h. (see Online Resource 12). Nonetheless, carbon transfer at lower humidity is not as prevalent as in tests carried out at ambient humidity. At low humidity only CNT5 shows prominent material transfer, with CNT3 and CNT4 showing marginal amounts of carbon transfer, where CNT3 shows slightly more material transfer than CNT4. This explains why the wear protection offered by CNT3 at 15% r.h. outperforms

CNT4 (see Fig. 7). Therefore, this confirms that wear protection is not strongly influenced by atmospheric humidity, but rather an aggregate of contact situation due to coating heterogeneity, amount of displaced coating, and amount of material transferred towards the counter electrode.

The counter electrodes used in the durability tests were also scanned via CLSM. In these cases, however, marginal traces of carbonaceous depositions can be observed; thus explaining why the wear protection offered by the coatings diminishes in these tests. For extended fretting tests, the prolonged shear stresses degrade the CNT and displace the carbon tribofilm from the contact site. The damaged CNT do not adhere to the counter electrode (see Online Resources 13 and 14), instead the graphitized particles are easily displaced from the contact site [10]. Consequently, wear protection is reduced with the bulk of transferred carbon being found at the ends of the fretting mark (as was observed in the fretting marks of the coated copper samples in Fig. 6).

4 Conclusions

In this work, three different CNT coatings were deposited over copper substrates. These coatings were tribo-electrically characterized to further understand the influence of coating thickness, the influence of normal load on fretting tests, and the wear reduction capabilities of CNT at low ambient humidity, taking into consideration the electrical behavior of the coated systems.

Thicker CNT coatings are not easily displaced by fretting at low normal loads, consequently, the ECR is higher than that of the uncoated copper. Nonetheless, for loads higher than 0.5 N this effect is negligible, albeit thicker coatings present higher ECR values than their thinner counterparts. From a tribological standpoint, thicker coatings promote smaller worn areas, with areal reductions between 80 and 90% in CNT5, for example. As expected, the wear protection offered by thinner coatings is reduced at higher normal loads. Therefore, the optimal coating thickness depends on the predominant objective, namely, electrical or tribological. Thinner coatings are preferred for applications where low ECR is crucial, with wear reduction being secondary. Whereas thicker coatings are required when improved tribological behavior is essential at the expense of conductivity.

For prolonged fretting cycles the CNT are displaced from the contacting site, with marginal carbon transfer towards the counter electrode. Consequently, the behavior of these coated samples resembles that of the uncoated. Therefore, in applications where prolonged fretting wear is expected these coatings do not contribute significant wear reduction. Nonetheless, if wear is not a key concern, low and stable ECR values were achieved for both 150 and 500 k fretting cycles, outperforming the uncoated reference samples.

At lower ambient humidity the wear protection of CNT is reduced, showing milder wear reduction compared to fretting tests carried out at ambient humidity. Furthermore, the electrical behavior also diminishes at lower humidity. The porous nature of the CNT coatings requires moderate contact pressures to enable compaction and readjustment of the coating. Contrarily, dry air located in the voids opposes a higher resistance than moist air, thus explaining the increased ECR at low humidity. Therefore, these coatings are not suitable for exclusive applications in low humidity. For applications where humidity fluctuates from ambient to below mean values (and vice versa), theses coatings show promising results as a versatile solid lubricant.

Supplementary Information The online version contains supplementary material available at https://doi.org/10.1007/s11249-023-01724-5.

Acknowledgements B. Alderete wishes to acknowledge the support from the German Academic Exchange Service (DAAD) and the Roberto Rocca Education Program (RREP). The TÜV Saarland Stiftung is gratefully acknowledged for financially supporting the project. The authors gratefully acknowledge funding in the ZuMat project, supported by the State of Saarland from the European Regional Development Fund (Europäischen Fonds für Regionale Entwicklung, EFRE). Funding for the PFIB/SEM instrument by German Research Foundation is greatly acknowledged (INST 256/510-1 FUGG).

Author Contributions Conceptualization: BA, SS; Methodology: BA, SS; Visualization: BA; Formal analysis and investigation: BA; Writing—original draft preparation: BA; Writing—review and editing: SS; Funding acquisition: FM, SS; Resources: FM; Supervision: FM, SS; Project Administration: FM, SS.

Funding Open Access funding enabled and organized by Projekt DEAL. The authors have not disclosed any funding.

Data availability Data available on request from the authors.

Declarations

Conflict of interest The authors have no relevant financial or non-financial interests to disclose.

References

1. Tsao, J.Y., Schubert, E.F., Fouquet, R., Lave, M.: The electrification of energy: long-term trends and opportunities. MRS Energy Sustain. (2018). https://doi.org/10.1557/mre.2018.6
2. Manzolli, J.A., Trovão, J.P., Antunes, C.H.: A review of electric bus vehicles research topics—Methods and trends. Renew Sustain Energy Rev (2022). https://doi.org/10.1016/j.rser.2022.112211
3. Zhou, E.M.T.: Electrification futures study: operational analysis of U.S. power systems with increased electrification and demand-side flexibility. Golden, Colorado (2021)
4. Varenberg, M., Etsion, I., Halperin, G.: Slip index: a new unified approach to fretting. Tribol Lett. **17**, 569–573 (2004). https://doi.org/10.1023/B:TRIL.0000044506.98760.f9
5. Slade, P.G.: Electrical contacts principles and applications. Taylor & Francis, Boca Raton (2014)
6. Hutchings, I.M., Shipway, P.: Tribology: Friction and wear of engineering materials. Butterworth-Heinemann (2017)
7. Varenberg, M., Etsion, I., Halperin, G.: Nanoscale fretting wear study by scanning probe microscopy. Tribol Lett. **18**, 493–498 (2005). https://doi.org/10.1007/s11249-005-3609-6
8. Antler, M., Drozdowicz, M.H.: Fretting corrosion of gold-plated connector contacts. Wear **74**, 27–50 (1981). https://doi.org/10.1016/0043-1648(81)90192-7
9. Trinh, K.E., Tsipenyuk, A., Varenberg, M., Rosenkranz, A., Souza, N., Mücklich, F.: Wear debris and electrical resistance in textured Sn-coated Cu contacts subjected to fretting. Wear **344–345**, 86–98 (2015). https://doi.org/10.1016/j.wear.2015.10.010
10. Alderete, B., Suarez, S., Tejeda, D.B., Mücklich, F.: Fretting and electrical contact resistance characteristics of carbon nanoparticle-coated Cu electrical contacts. In: 2022 IEEE 67th Holm Conference on Electrical Contacts (HLM). pp. 1–8. IEEE (2022)
11. Falcao, E.H.L., Wudl, F.: Carbon allotropes: beyond graphite and diamond. J. Chem. Technol. Biotechnol. **82**, 524–531 (2007). https://doi.org/10.1002/jctb.1693
12. Hirsch, A.: The era of carbon allotropes. Nat Mater. **9**, 868–871 (2010). https://doi.org/10.1038/nmat2885
13. Alderete, B., Mücklich, F., Suarez, S.: Characterization and electrical analysis of carbon-based solid lubricant coatings. Carbon Trends (2022). https://doi.org/10.1016/j.cartre.2022.100156
14. Reinert, L., Lasserre, F., Gachot, C., Grützmacher, P., MacLucas, T., Souza, N., Mücklich, F., Suarez, S.: Long-lasting solid lubrication by CNT-coated patterned surfaces. Sci Rep. **7**, 1–13 (2017). https://doi.org/10.1038/srep42873
15. Reinert, L., Green, I., Gimmler, S., Lechthaler, B., Mücklich, F., Suàrez, S.: Tribological behavior of self-lubricating carbon nanoparticle reinforced metal matrix composites. Wear **408–409**, 72–85 (2018). https://doi.org/10.1016/j.wear.2018.05.003
16. Reinert, L., Suarez, S., Rosenkranz, A.: Tribo-mechanisms of carbon nanotubes: friction and wear behavior of CNT-reinforced nickel matrix composites and CNT-coated bulk nickel. Lubricants. **4**, 11 (2016). https://doi.org/10.3390/lubricants4020011
17. MacLucas, T., Suarez, S.: On the solid lubricity of electrophoretically deposited carbon nanohorn coatings. Lubricants. **7**, 60 (2019). https://doi.org/10.3390/lubricants7080062
18. Zhmud, B., Pasalskiy, B.: Nanomaterials in lubricants: an industrial perspective on current research. Lubricants. **1**, 95–101 (2013). https://doi.org/10.3390/lubricants1040095
19. Saito, R., Dresselhaus, G., Dresselhaus, M.S.: Physical properties of carbon nanotubes. Imperial College Press, London (1998)
20. Dresselhaus, M.S., Dresselhaus, G., Saito, R.: Physics of carbon nanotubes. Carbon NY. **33**, 883–891 (1995). https://doi.org/10.1016/0008-6223(95)00017-8
21. Popov, V.N.: Carbon nanotubes: Properties and application. Mater. Sci. Eng. R. Rep. **43**, 61–102 (2004). https://doi.org/10.1016/j.mser.2003.10.001
22. Ebbesen, T.W.: Carbon nanotubes. Chem Eng News. **79**, 11 (2001)
23. Saifuddin, N., Raziah, A.Z., Junizah, A.R.: Carbon nanotubes: a review on structure and their interaction with proteins. J Chem. **2013**, 18 (2013). https://doi.org/10.1155/2013/676815
24. Nasir, S., Hussein, M.Z., Zainal, Z., Yusof, N.A.: Carbon-based nanomaterials/allotropes: a glimpse of their synthesis, properties and some applications. Materials. **11**, 1–24 (2018). https://doi.org/10.3390/ma11020295
25. Ando, T., Matsumura, H., Nakanishi, T.: Theory of ballistic transport in carbon nanotubes. Physica B. **323**, 44–50 (2002)
26. Svizhenko, A., Anantram, M.P., Govindan, T.R.: Ballistic transport and electrostatics in metallic carbon nanotubes. IEEE Trans Nanotechnol. **4**, 557–562 (2005). https://doi.org/10.1109/TNANO.2005.851409
27. Li, H.J., Lu, W.G., Li, J.J., Bai, X.D., Gu, C.Z.: Multichannel ballistic transport in multiwall carbon nanotubes. Phys Rev Lett. (2005). https://doi.org/10.1103/PhysRevLett.95.086601
28. van der Veen, M.H., Barbarin, Y., Kashiwagi, Y., Tokei, Z.: Electron mean-free path for CNT in vertical interconnects approaches Cu. In: 2014 IEEE International Interconnect Technology Conference/Advanced Metallization Conference, IITC/AMC 2014. pp. 181–184. IEEE Computer Society (2014)
29. Maiti, A., Svizhenko, A., Anantram, M.P.: Electronic transport through carbon nanotubes: effects of structural deformation and tube chirality. Phys Rev Lett. **88**, 4 (2002). https://doi.org/10.1103/PhysRevLett.88.126805
30. Yanagi, K., Udoguchi, H., Sagitani, S., Oshima, Y., Takenobu, T., Kataura, H., Ishida, T., Matsuda, K., Maniwa, Y.: Transport mechanisms in metallic and semiconducting single-wall carbon nanotube networks. ACS Nano **4**, 4027–4032 (2010). https://doi.org/10.1021/nn101177n
31. Krupke, R., Hennrich, F., Löhneysen, H.V., Kappes, M.M.: Separation of metallic from semiconducting single-walled carbon nanotubes. Science. **301**, 344–347 (2003). https://doi.org/10.1126/science.1086534
32. Li, H., Yin, W.Y., Banerjee, K., Mao, J.F.: Circuit modeling and performance analysis of multi-walled carbon nanotube interconnects. IEEE Trans Electron Devices. **55**, 1328–1337 (2008). https://doi.org/10.1109/TED.2008.922855
33. Robertson, J., Zhong, G., Hofmann, S., Bayer, B.C., Esconjauregui, C.S., Telg, H., Thomsen, C.: Use of carbon nanotubes for VLSI interconnects. Diam Relat Mater. **18**, 957–962 (2009). https://doi.org/10.1016/j.diamond.2009.02.008
34. Suarez, S.: Development of carbon nanotube-reinforced nickel matrix composites: processing, microstructure and physical properties (2014)
35. Berman, D., Erdemir, A., Sumant, A.V.: Graphene: a new emerging lubricant. Materials Today **17**, 31–42 (2014)
36. Scharf, T.W., Prasad, S. V.: Solid lubricants: a review (2013)
37. Chen, Z., He, X., Xiao, C., Kim, S.H.: Effect of humidity on friction and wear—a critical review (2018)
38. Morstein, C.E., Klemenz, A., Dienwiebel, M., Moseler, M.: Humidity-dependent lubrication of highly loaded contacts by graphite and a structural transition to turbostratic carbon. Nat Commun. (2022). https://doi.org/10.1038/s41467-022-33481-9
39. Lancaster, J.K.: A review of the influence of environmental humidity and water on friction, lubrication and wear. Tribol Int. **23**, 371–389 (1990). https://doi.org/10.1016/0301-679X(90)90053-R
40. de Wijn, A.S., Fasolino, A., Filippov, A.E., Urbakh, M.: Low friction and rotational dynamics of crystalline flakes in solid lubrication. EPL. (2011). https://doi.org/10.1209/0295-5075/95/66002

41. Langlade, C., Fayeulle, S., Olier, R.: New insights into adhesion and lubricating properties of graphite-based transfer films. Wear **172**, 85–92 (1994). https://doi.org/10.1016/0043-1648(94)90303-4
42. Ouyang, J.H., Li, Y.F., Zhang, Y.Z., Wang, Y.M., Wang, Y.J.: High-temperature solid lubricants and self-lubricating composites: a critical review (2022)
43. Lepage, J., Zaida, H.: Influence of the water vapour adsorption on the boundary conditions in tribology. Tribol Ser. **12**, 259–266 (1987). https://doi.org/10.1016/S0167-8922(08)71074-5
44. Kumar, R., Hussainova, I., Rahmani, R., Antonov, M.: Solid lubrication at high-temperatures—a review (2022)
45. Lijima, S.: Helical microtubules of graphitic carbon. Nature. **354**, 56–58 (1991)
46. Reinert, L., Schütz, S., Suárez, S., Mücklich, F.: Influence of surface roughness on the lubrication effect of carbon nanoparticle-coated steel surfaces. Tribol Lett. **66**, 1–11 (2018). https://doi.org/10.1007/s11249-018-1001-6
47. Greenberg, R., Halperin, G., Etsion, I., Tenne, R.: The effect of WS_2 nanoparticles on friction reduction in various lubrication regimes. Tribol Lett. **17**, 179–186 (2004). https://doi.org/10.1023/B:TRIL.0000032443.95697.1d
48. MacLucas, T., Klemenz, A., Grünewald, P., Presser, V., Mayrhofer, L., Moras, G., Suarez, S., Dienwiebel, M., Mücklich, F., Moseler, M.: Multiwall carbon nanotubes for solid lubrication of highly loaded contacts. ACS Appl Nano Mater. (2023). https://doi.org/10.1021/acsanm.2c04729
49. Alderete, B., MacLucas, T., Espin, D., Brühl, S.P., Mücklich, F., Suarez, S.: Near superhydrophobic carbon nanotube coatings obtained via electrophoretic deposition on low-alloy steels. Adv Eng Mater. (2021). https://doi.org/10.1002/adem.202001448
50. Alderete, B., Lößlein, S.M., Bucio Tejeda, D., Mücklich, F., Suarez, S.: Feasibility of carbon nanoparticle coatings as protective barriers for copper─wetting assessment. Langmuir (2022). https://doi.org/10.1021/acs.langmuir.2c02295
51. Alderete, B., Puyol, R., Slawik, S., Espin, E., Mücklich, F., Suarez, S.: Multipurpose setup used to characterize tribo-electrical properties of electrical contact materials. MethodsX. (2021). https://doi.org/10.1016/j.mex.2021.101498
52. Woo Park, Y., Sankara Narayanan, T.S.N., Yong Lee, K.: Effect of fretting amplitude and frequency on the fretting corrosion behaviour of tin plated contacts. Surf Coat Technol. **201**, 2181–2192 (2006). https://doi.org/10.1016/j.surfcoat.2006.03.031
53. Bock, E.M.: Low-level contact resistance characterization. AMP J Technol. **3**, 64–68 (1993)
54. Platzman, I., Brener, R., Haick, H., Tannenbaum, R.: Oxidation of polycrystalline copper thin films at ambient conditions. J. Phys. Chem. C **112**, 1101–1108 (2008). https://doi.org/10.1021/jp076981k
55. Tsai, J.T.H., Lu, C.C., Li, J.G.: Fabrication of humidity sensors by multi-walled carbon nanotubes. J Exp Nanosci. **5**, 302–309 (2010). https://doi.org/10.1080/17458080903513300
56. Lee, Y., Yoon, J., Kim, Y., Kim, D.M., Kim, D.H., Choi, S.J.: Humidity effects according to the type of carbon nanotubes. IEEE Access. **9**, 6810–6816 (2021). https://doi.org/10.1109/ACCESS.2020.3048173
57. Ling, Y., Gu, G., Liu, R., Lu, X., Kayastha, V., Jones, C.S., Shih, W.S., Janzen, D.C.: Investigation of the humidity-dependent conductance of single-walled carbon nanotube networks. J Appl Phys. (2013). https://doi.org/10.1063/1.4774075
58. Shamai, R., Andelman, D., Berge, B., Hayes, R.: Water, electricity, and between on electrowetting and its applications. Soft Matter **4**, 38–45 (2007). https://doi.org/10.1039/b714994h
59. Quinn, A., Sedev, R., Ralston, J.: Contact angle saturation in electrowetting. J. Phys. Chem. B **109**, 6268–6275 (2005). https://doi.org/10.1021/jp040478f
60. Frick, C., Steiner, H., Mazurkiewicz, A., Riediger, U., Rauthe, M., Reich, T., Gratzki, A.: Central European high-resolution gridded daily data sets (HYRAS): mean temperature and relative humidity. Meteorol. Z. **23**, 15–32 (2014). https://doi.org/10.1127/0941-2948/2014/0560
61. Sachindra, D.A., Nowosad, M.: Variations in relative humidity across Poland and its possible impacts on outdoor thermal comfort: an analysis based on hourly data from 1995 to 2020. Int. J. Climatol. **42**, 3861–3887 (2022). https://doi.org/10.1002/joc.7449
62. Vingsbo, O., Söderberg, S.: On fretting maps. Wear **126**, 131–147 (1988). https://doi.org/10.1016/0043-1648(88)90134-2
63. Varenberg, M., Halperin, G., Etsion, I.: Different aspects of the role of wear debris in fretting wear. Wear **252**, 902–910 (2002)
64. Reinert, L., Varenberg, M., Mücklich, F., Suárez, S.: Dry friction and wear of self-lubricating carbon-nanotube-containing surfaces. Wear **406–407**, 33–42 (2018). https://doi.org/10.1016/j.wear.2018.03.021
65. Jian, S.R., Chen, G.J., Hsu, W.M.: Mechanical properties of Cu2O thin films by nanoindentation. Materials. **6**, 4505–4513 (2013). https://doi.org/10.3390/ma6104505

Authors and Affiliations

Bruno Alderete[1] · Frank Mücklich[1] · Sebastian Suarez[1]

✉ Bruno Alderete
bruno.alderete@uni-saarland.de

[1] Chair of Functional Materials, Saarland University, Campus D3.3, 66123 Saarbrücken, Germany